Novel Astronomical Probes of Axions

with photon "baselines" of kpc, Mpc, and Gpc

Chen Sun

Tel Aviv University

Buen-Abad, Fan, CS, 2110.13916 & 2011.05993

Things that I won't talk about –

- review of the cosmological constraints of FIPs →c.f. Wallisch's talk
- review of the astrophysical constraints of FIPs → c.f. Carenza's talk
- Israel election, US midterm, etc.

$$g_{a\gamma} a F\tilde{F} \sim g_{a\gamma} a \ \mathbf{E} \cdot \mathbf{B}$$

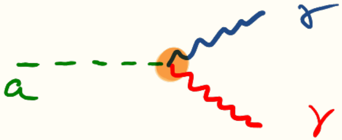

$$\Gamma_a \sim g_{a\gamma}^2 m_a^3$$

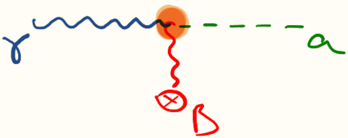

$$P_{\gamma\to a} \sim (g_{a\gamma} B L)^2$$

$$g_{a\gamma} a F\tilde{F} \sim g_{a\gamma} a \, \mathbf{E} \cdot \mathbf{B}$$

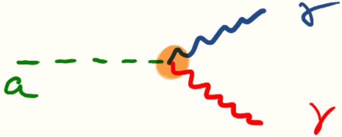

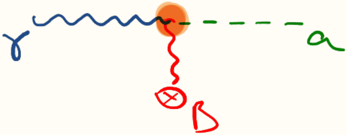

$$\Gamma_a \sim g_{a\gamma}^2 m_a^3 \qquad\qquad P_{\gamma\to a} \sim (g_{a\gamma} B L)^2$$

Because we know $g_{a\gamma}$ is tiny (below $\mathcal{O}(10^{-11})\mathrm{GeV}^{-1}$ from CAST, Superstar clusters, NGC1275, CMB spectral distortion, SN explosion ...)

- enhance the decay rate suppressed by the phase space.
- maximize $(B \times L)$ by strong B or large L,

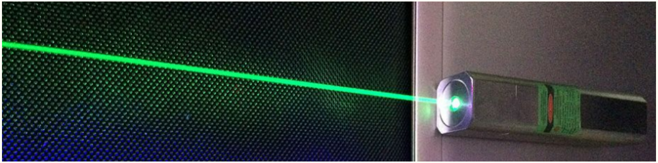

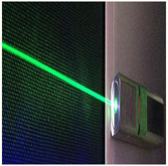

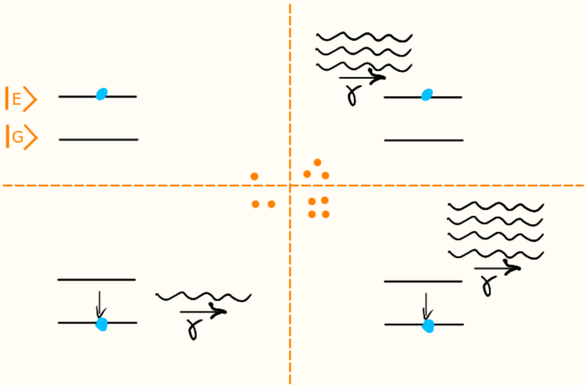

|E⟩
|G⟩
γ
γ
γ

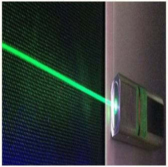

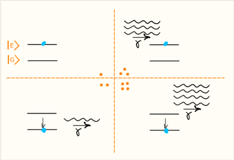

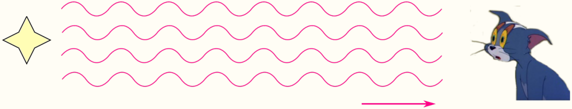

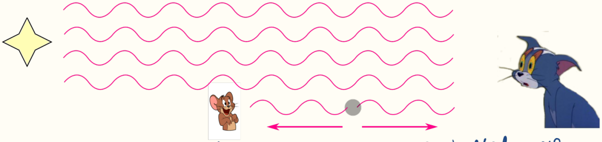

Arza & Sikivie . 2019
Arza & Todarello 2021

Caputo et al. 2018 .

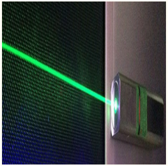

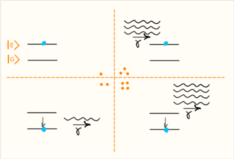

|E⟩
|G⟩

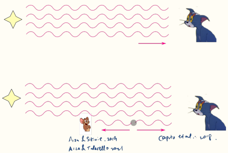

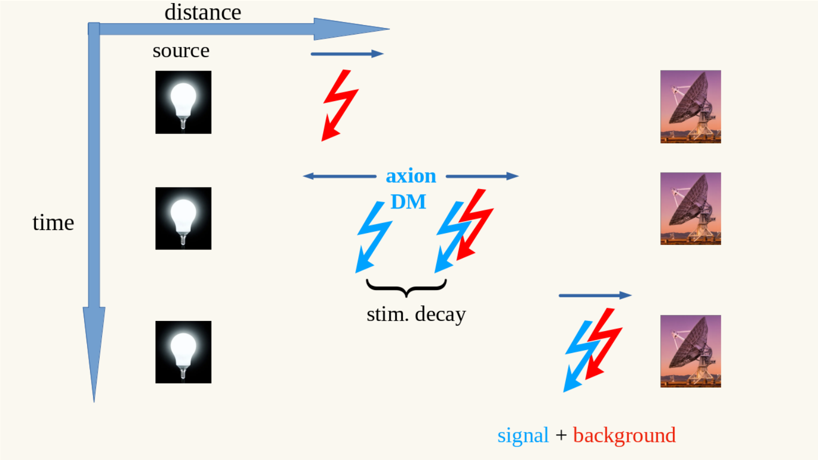

distance
source
time
axion
DM
stim. decay
signal + background

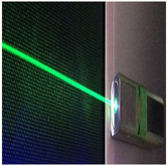

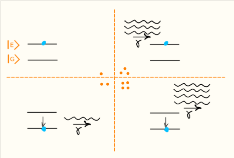

|E⟩
|G⟩

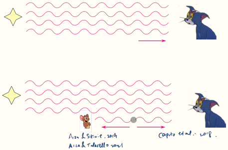

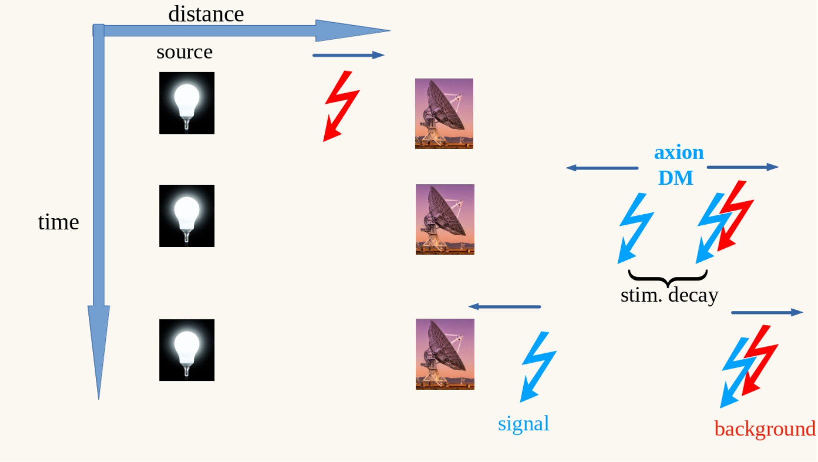

distance
source
time
axion
DM
stim. decay
signal
background

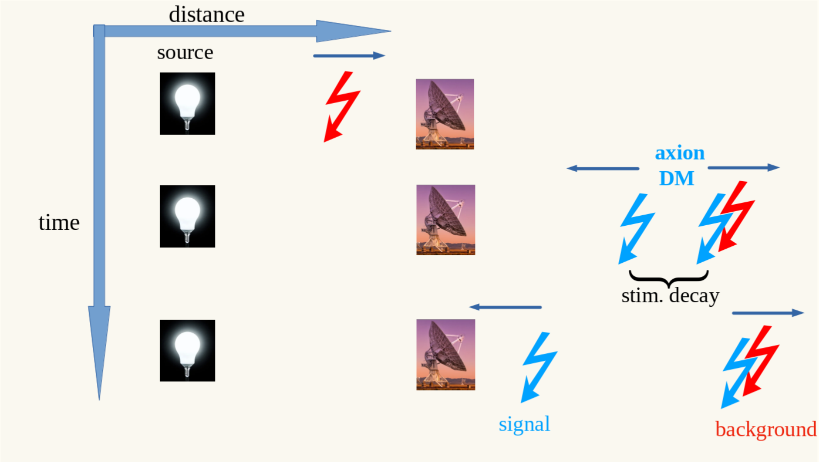

- Forward signal: arrives together with γ triggering the decay
- Backward signal:
  - separated from γ that generate them
  - not directly related to the radio source brightness at detection time candidates: galactic supernova remnants $\sim$O(1000) yo

signal flux density

[power/area/freq]

$$S_{\nu_a} = \frac{16\pi^2\Gamma_a}{m_a^4\,\sigma_a}\int dx\,\rho_a\,S_{\nu_a,stim}$$

line width $\sim 10^{-3}(m_a/4\pi)$

$$P_{\rm signal} = S_\nu \cdot \Delta\nu \cdot A \cdot \eta$$

telescope efficiency

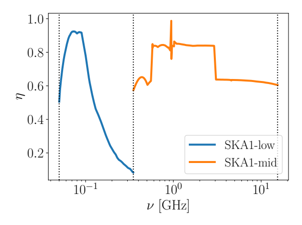

telescope area

$\sum$ (unit area)

Signal/ Noise

$$P_{\rm noise,inst} = T_{\rm sys}\,\Delta\nu$$

- $T_{\rm cmb} \approx 2.73$ K
- $T_{\rm atm} \approx 3$ K at 1 GHz, $\sim \mathcal{O}(100)$ K at 100 MHz.
- $T_{\rm gal} \sim \mathcal{O}(10)$ K (inhomogeneous, Haslam 408 MHz map),
- $T_{\rm rcv} \approx 40$ K for SKA-low, and $T_{\rm r} \sim \mathcal{O}(10)$ K for SKA-mid
- $T_{\rm spl} \lesssim 3$ K

Signal/ Noise

$$P_{\text{noise}} = \frac{\sum_{\text{units}} \left(T_{\text{sys}}\,\Delta\nu\right)}{\left(\#\text{ of meas.}\right)^{1/2}}$$

- $\sum_{\text{units}}$ is over all stations/dishes that receives the signal
- (# of meas.) is the number of independent measurements
  - 2 polarizations
  - $(\Delta\nu\, t_{\text{obs}})$ during t_{obs}
  - # of dishes (single-dish mode)
  - # of baselines (interferometry mode)

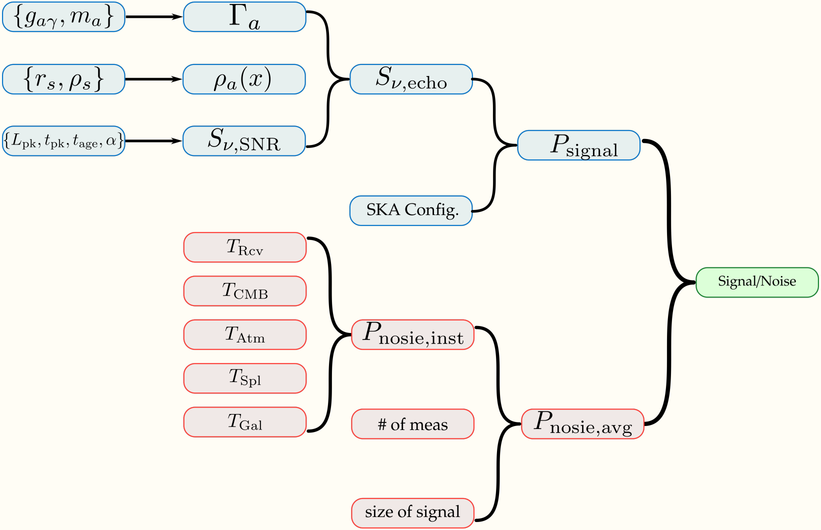
$\{g_{a\gamma}, m_a\}$
$\{r_s, \rho_s\}$
$\{L_{pk}, t_{pk}, t_{age}, \alpha\}$
Γ_a
$\rho_a(x)$
$S_{\nu,SNR}$
$S_{\nu,echo}$
SKA Config.
P_{signal}
T_{Rcv}
T_{CMB}
T_{Atm}
T_{Spl}
T_{Gal}
$P_{nosie,inst}$
# of meas
size of signal
$P_{nosie,avg}$
Signal/Noise

G39.7-2.0 (W50)
$(l, b) = (39.7^\circ, -2^\circ)$
$\theta_\mathrm{s} = 85$ arcmin
$S^{(0)}_{1\mathrm{GHz,s}} = 85$ Jy $(*)$
$D = 4.9$ kpc
$t_\mathrm{age} = 30,000$–$100,000$ years
$\alpha = 0.7\ (*)$
$\gamma = 1.92$

G39.7-2.0 (W50)
$(l, b) = (39.7^\circ, -2^\circ)$
$\theta_s = 85$ arcmin
$S^{(0)}_{1\mathrm{GHz,s}} = 85$ Jy $(*)$
$D = 4.9$ kpc
$t_{\mathrm{age}} = 30,000$–$100,000$ years
$\alpha = 0.7$ $(*)$
$\gamma = 1.92$

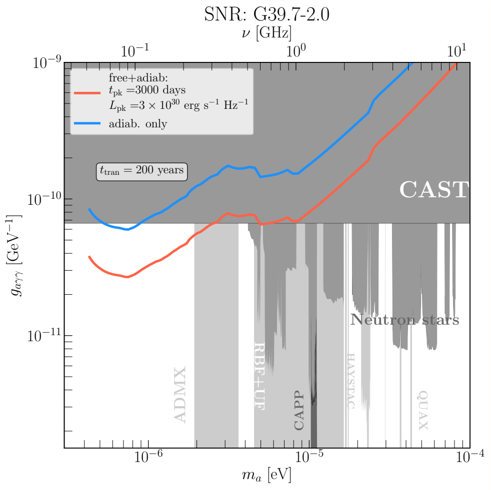

Buen-Abad, Fan, **CS** 2110.13916
also see Schutz et al. 2110.13920

G6.4-0.1 like
$(l, b) = (64^\circ, -0.1^\circ)$
$\theta_s = 48$ arcmin
$S^{(0)}_{1\mathrm{GHz,s}} = 310$ Jy $(*)$
$D = 1.9$ kpc
$t_{\mathrm{age}} \sim 35,000$ years
$\alpha = 0.65$ $(*)$
$\gamma = 1.84$
$t_{\mathrm{pk}} = t_{\mathrm{tran}}/30$

G6.4-0.1 like
$(l, b) = (64^\circ, -0.1^\circ)$
θ_s = 48 arcmin
$S^{(0)}_{1\mathrm{GHz,s}}$ = 310 Jy $(*)$
D = 1.9 kpc
$t_{\mathrm{age}} \sim 35{,}000$ years
$\alpha = 0.65$ $(*)$
$\gamma = 1.84$
$t_{\mathrm{pk}} = t_{\mathrm{tran}}/30$

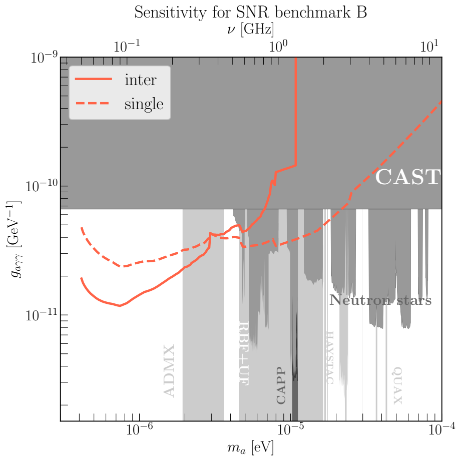

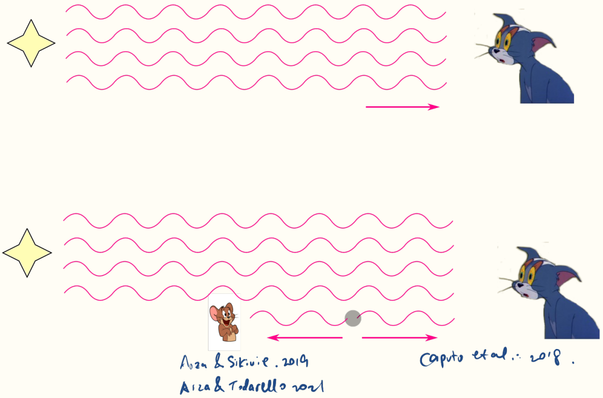
Arza & Sikivie . 2019
Arza & Todarello 2021
Caputo et al. 2018 .

$\gamma - a$ oscillation in the cosmological context

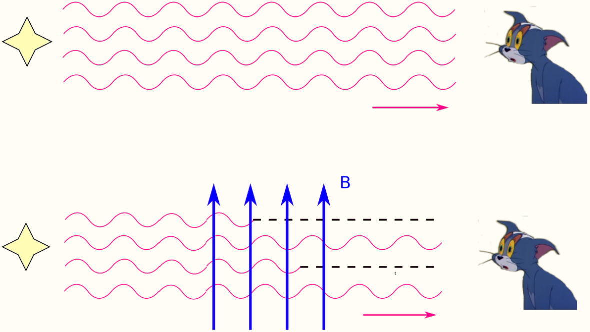

Mpc

angular size

physical size

$$\theta \sim \frac{\ell}{D_A}$$

angular diameter distance

- $\gamma - a$ oscillation won't affect D_A if ℓ is known (std ruler)
- Some objects have unknown size ℓ, which can only be inferred from their brightness measurement

Galaxy Clusters

Observable:

- X-ray surface brightness

$$S_X \propto \int n_e^2 \Lambda_{ee} d\ell = \int n_e^2 \Lambda_{ee} D_A d\theta$$

- Sunyaev-Zel'dovich Effect (SZE)

$$\Delta T_{CMB} \propto \int n_e T_e d\ell = \int n_e T_e D_A d\theta$$

$$D_A \propto \frac{\Delta T_{CMB}^2}{S_X}$$

$D_A \propto \frac{\Delta T_{CMB}^2}{S_X}$

With axions, the observables are affected as

$$\Delta T_{CMB} \to \Delta T_{CMB} \times P_{\gamma\gamma}^{IGM}(\omega_{CMB})$$
$$S_X \to S_X \times P_{\gamma\gamma}^{IGM}(\omega_X) \langle P_{\gamma\gamma}^{ICM}(\omega_X) \rangle$$

which leads to a modification of the angular diameter distance

$$D_A \to D_A \times \frac{P_{\gamma\gamma}^{IGM}(\omega_{CMB})^2}{P_{\gamma\gamma}^{IGM}(\omega_X)} \langle P_{\gamma\gamma}^{ICM}(\omega_X) \rangle$$

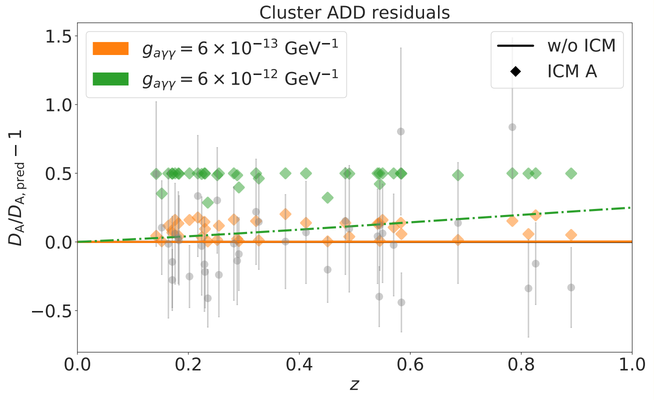

$$D_A \to D_A \times \frac{P_{\gamma\gamma}^{IGM}(\omega_{CMB})^2}{P_{\gamma\gamma}^{IGM}(\omega_X)} \langle P_{\gamma\gamma}^{ICM}(\omega_X) \rangle$$

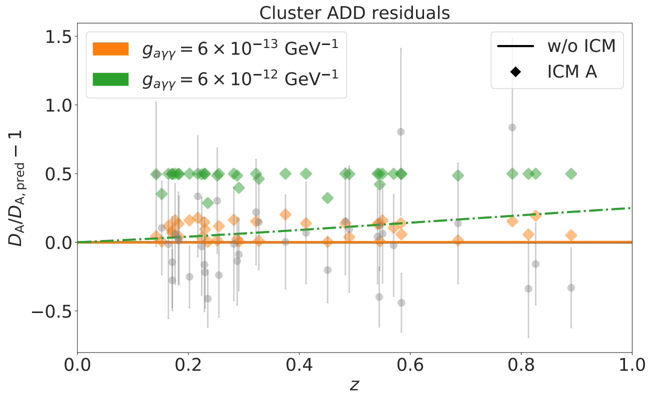

$$-2 \ln \mathcal{L}_{cl} = \sum_{i=1}^{38} \left(\frac{D_{A,i}^{exp} - D_A^{th}(z_i; \theta)}{\sigma_i^{exp}} \right)^2$$

Gpc

$$F = \frac{L}{4\pi {D_L}^2},$$

Type Ia supernova

$$F = P_{\gamma\gamma}(D_L)\frac{L}{4\pi {D_L}^2},$$

- Measure $F, D_L \Rightarrow L$ "anchor"
- Measure $F \Rightarrow P_{\gamma\gamma}(D_L)/D_L^2$

Type Ia supernova

$$F = P_{\gamma\gamma}(D_L)\frac{L}{4\pi {D_L}^2},$$

- Measure $F, D_L \Rightarrow L$ "anchor"
- Measure $F \Rightarrow P_{\gamma\gamma}(D_L)/D_L^2$

- The $a-\gamma$ conversion modifies how we map flux F to the lum distance D_L. The shape of $F(D_L)$ is modified
- In a ΛCDM universe, $D_L = D_L(z;\ \Lambda, H_0) \Rightarrow$ flux-redshift relation. Shape of $F(z; g_{a\gamma}, \Lambda)$ can be constrained by SNIa data set
- $g_{a\gamma}$ degenerates with Λ, but if If Λ is anchored by an external data set, e.g. BAO or galaxy clusters, the constrain on $F(z)$ is a constraint on $g_{a\gamma}$

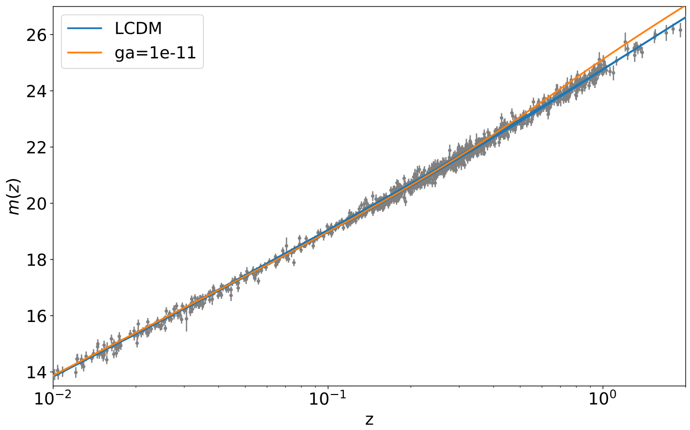
LCDM
ga=1e-11
26
24
22
20
18
16
14
m(z)
10^{-2}
10^{-1}
10^{0}
z

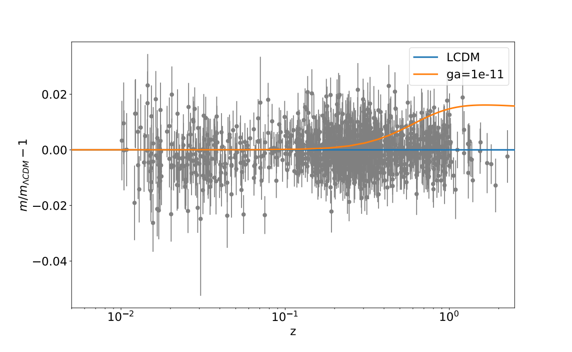

The likelihood:

$$-2\ln\mathcal{L}_{Pan} = \sum_{i,j=1}^{1048}\left(m_i^{Pan} - m^{th}(z_i;\theta,M)\right)C_{ij}^{Pan}\left(m_j^{Pan} - m^{th}(z_j;\theta,M)\right)$$

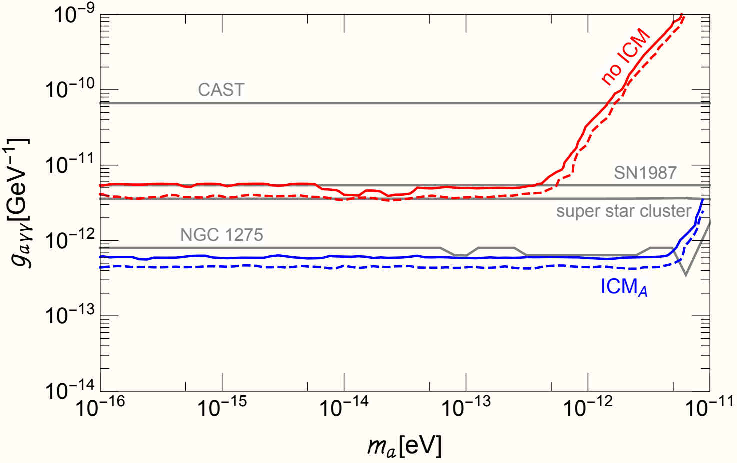

10^{-9}
10^{-10}
10^{-11}
10^{-12}
10^{-13}
10^{-14}
10^{-16}
10^{-15}
10^{-14}
10^{-13}
10^{-12}
10^{-11}
$g_{a\gamma\gamma}$[GeV^{-1}]
m_a[eV]
CAST
no ICM
SN1987
super star cluster
NGC 1275
ICM$_A$

Summary

- There is rich phenomenology in the propagation of photons emitted by natural sources, induced by axion or axion DM.

  · high photon occupation number · magnetic field · long baselines

- kpc: DM $a \to \gamma_f + \gamma_b$ leads to echo signals from transient sources (that are dim today) by the stimulated decay

  thanks to the large γ_f occupation number;

  γ_b depends on historical source brightness; has low background;

- Mpc: $\gamma \to a$ in B_{ICM} modifies distance inference of galaxy clusters

  introduce a cluster dependence to the reconstructed Hubble diagram.

- Gpc: $\gamma \to a$ in B_{IGM} modifies distance inference of SNIa,

  introduce an extra redshift dependence to the Hubble diagram.

https://github.com/ChenSun-Phys/cosmo_axions
https://github.com/ChenSun-phys/snr_ghosts

Backup slides

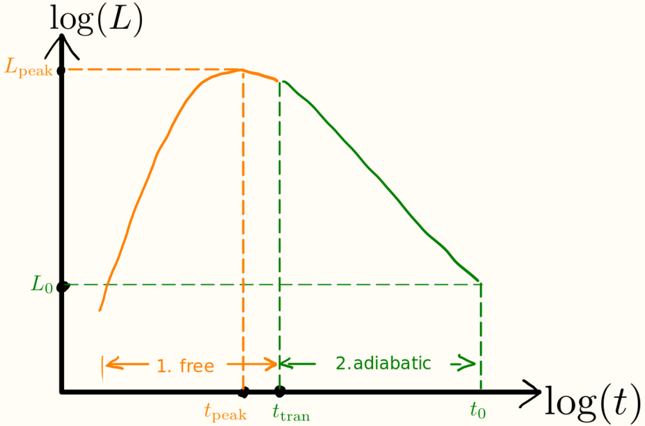

$\log(L)$
L_{peak}
L_0
1. free
2.adiabatic
t_{peak}
t_{tran}
t_0
$\log(t)$

$$L(t) = L_{\rm peak}\, e^{1.5(1-t_{\rm peak}/t)} \left(\frac{t}{t_{\rm peak}}\right)^{-1.5},$$

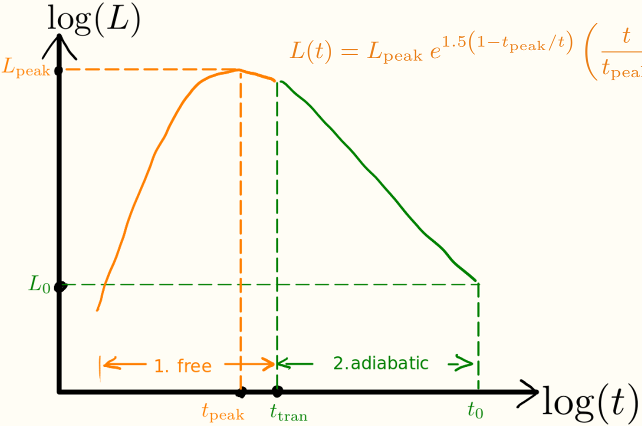

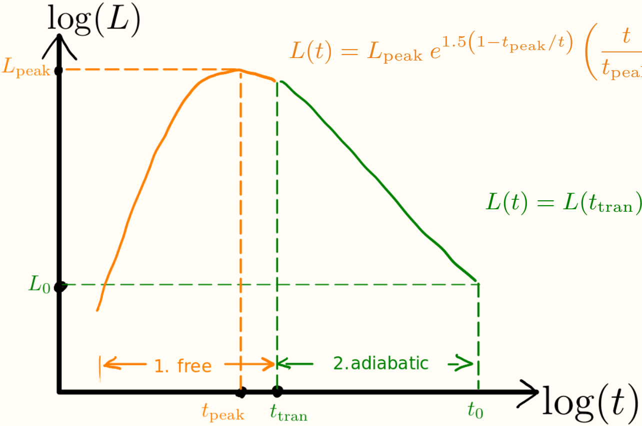

$$L(t) = L_{\rm peak}\, e^{1.5(1-t_{\rm peak}/t)} \left(\frac{t}{t_{\rm peak}}\right)^{-1.5},$$

$$L(t) = L(t_{\rm tran}) \left(\frac{t}{t_{\rm tran}}\right)^{-\gamma}$$

Phases of SNR Evolution

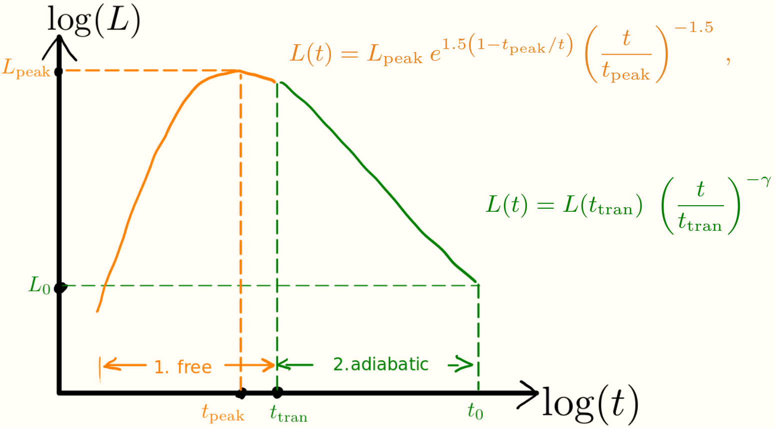

- 1. Free expansion, $\sim \mathcal{O}(100)$ yr
- 2. Adiabatic, $\sim \mathcal{O}(10^4)$ yr
- 3. Snow plough, $\sim \mathcal{O}(10^5)$ yr
- 4. Dispersion phase, $\sim \mathcal{O}(10^6)$ yr

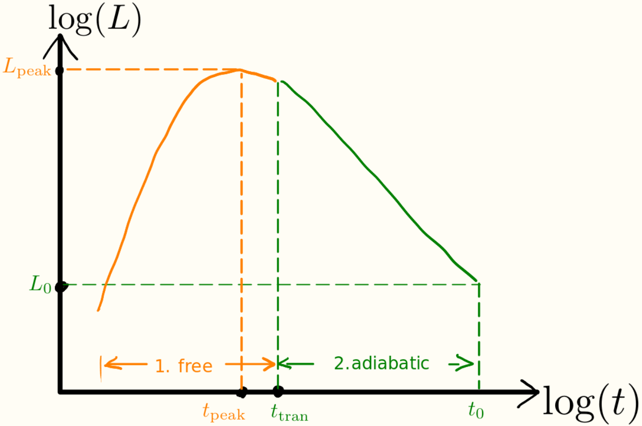

$\log(L)$
L_{peak}
L_0
1. free
2.adiabatic
t_{peak}
t_{tran}
t_0
$\log(t)$

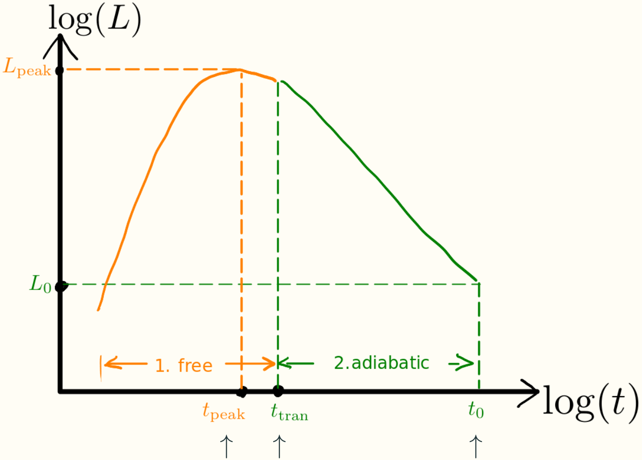

shape parameter

← We can anchor with L_{peak}

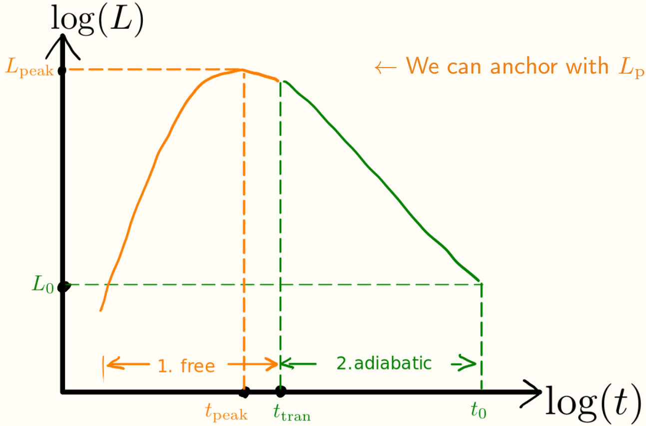

↑ ↑ ↑

shape parameter

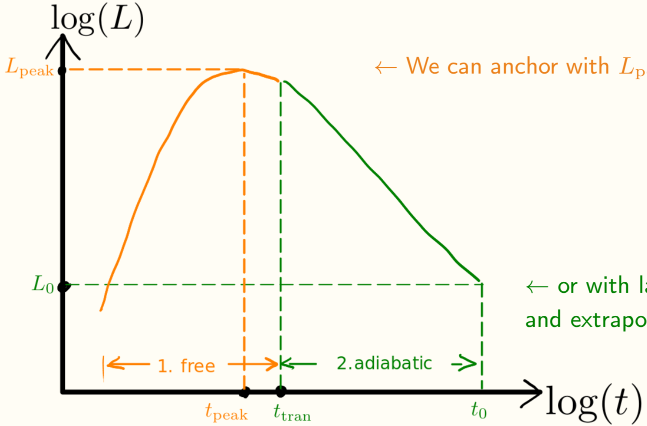

← We can anchor with $L_{\rm peak}$

← or with late time L_0, and extrapolate backward

↑ ↑ ↑

shape parameter

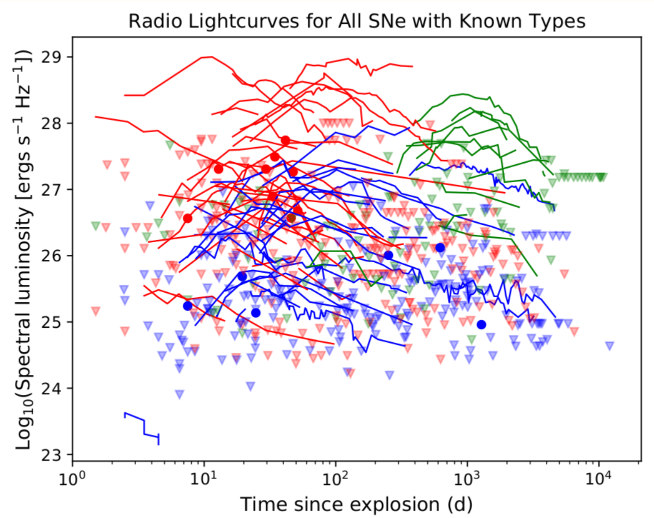

Radio Lightcurves for All SNe with Known Types
Log10(Spectral luminosity [ergs s−1 Hz−1])
29
28
27
26
25
24
23
10^0
10^1
10^2
10^3
10^4
Time since explosion (d)

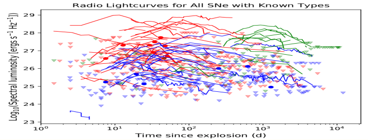
Radio Lightcurves for All SNe with Known Types
Time since explosion (d)

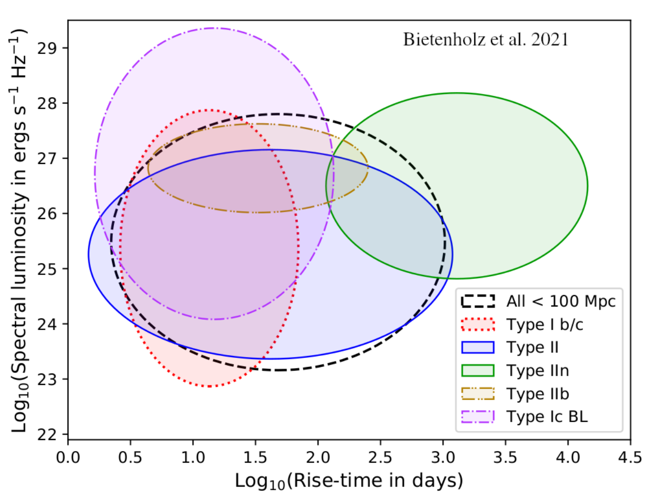
Bietenholz et al. 2021
Log10(Spectral luminosity in ergs s−1 Hz−1)
Log10(Rise-time in days)
All < 100 Mpc
Type I b/c
Type II
Type IIn
Type IIb
Type Ic BL

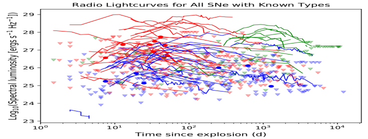

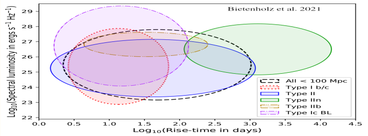

Green 2019

Table 1. 294 Galactic supernova remnants: summary data.

l	b	RA (J2000) (h m s)	Dec (° ′)	size /arcmin	type	Flux at 1 GHz/Jy	spectral index	other name(s)
0.0	+0.0	17 45 44	−29 00	3.5×2.5	S	100?	0.8?	Sgr A East
0.3	+0.0	17 46 15	−28 38	15×8	S	22	0.6	
0.9	+0.1	17 47 21	−28 09	8	C	18?	varies	
1.0	−0.1	17 48 30	−28 09	8	S	15	0.6?	
1.4	−0.1	17 49 39	−27 46	10	S	2?	?	
1.9	+0.3	17 48 45	−27 10	1.5	S	0.6	0.6	
3.7	−0.2	17 55 26	−25 50	14×11	S	2.3	0.65	
3.8	+0.3	17 52 55	−25 28	18	S?	3?	0.6	
4.2	−3.5	18 08 55	−27 03	28	S	3.2?	0.6?	
4.5	+6.8	17 30 42	−21 29	3	S	19	0.64	Kepler, SN1604,
4.8	+6.2	17 33 25	−21 34	18	S	3	0.6	
5.2	−2.6	18 07 30	−25 45	18	S	2.6?	0.6?	
5.4	−1.2	18 02 10	−24 54	35	C?	35?	0.2?	Milne 56
5.5	+0.3	17 57 04	−24 00	15×12	S	5.5	0.7	
5.9	+3.1	17 47 20	−22 16	20	S	3.3?	0.4?	
6.1	+0.5	17 57 29	−23 25	18×12	S	4.5	0.9	
6.1	+1.2	17 54 55	−23 05	30×26	F	4.0?	0.3?	
6.4	−0.1	18 00 30	−23 26	48	C	310	varies	W28
6.4	+4.0	17 45 10	−21 22	31	S	1.3?	0.4?	
6.5	−0.4	18 02 11	−23 34	18	S	27	0.6	
7.0	−0.1	18 01 50	−22 54	15	S	2.5?	0.5?	
7.2	+0.2	18 01 07	−22 38	12	S	2.8	0.6	

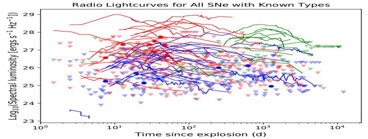

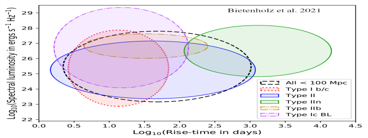

Green 2019

Table 1. 294 Galactic supernova remnants: summary data.

l	*b*	RA (J2000) (h m s)	Dec (° ′)	size /arcmin	type	Flux at 1 GHz/Jy	spectral index	other name(s)
0.0	+0.0	17 45 44	−29 00	3.5×2.5	S	100?	0.8?	Sgr A East

SNRcat - *High Energy Observations of Galactic Supernova Remnants*

Image (GAL alignment)	ID	names	context	age (years)	distance (kpc)	type	keV	MeV	GeV	TeV	CHANDRA	XMM
							all	all	all	all	all	all
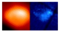	G000.0+00.0	Sgr A East, *CXOGC J174545.5-285829, 1FGL J1745.6-2900c, 2FGL J1745.6-2858, 1FHL J1745.6-2900, 3FGL J1745.6-2859c, 2FHL J1745.7-2900, 3FHL J1745.6-2900, HESS J1745-290, VER J1745-290*	contains CXOGC J174545.5-285829 = the Cannonball = NS candidate and possibly PWN, close to BH Sgr A* interacts with molecular cloud	1200 - 10000	8	thermal composite	keV		GeV	TeV	CHANDRA	XMM
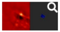	G000.1-00.1	G0.13-0.12, *1FGL J1746.4-2849c, 2FGL J1746.6-2851c, 1FHL J1746.3-2851, 3FGL J1746.3-2851c, VER J1746-289*	contains PWN G0.13-0.11 interacts with molecular cloud??			thermal & plerionic composite?	keV		GeV	TeV	CHANDRA	XMM
	G000.3+00.0	~~G0.33+0.04~~, ~~G0.4+0.1~~		≤ 500000	8.5	shell			GeV	TeV		
			contains PSR									

Early phase: statistics of 262 SNe measured in the range of 2-10 GHz leads to

$$L_{\text{peak}} = 10^{1.7\pm0.9}\text{erg s}^{-1}\ \text{Hz}^{-1}, \qquad t_{\text{peak}} = 10^{25.5\pm1.5}\ \text{d}$$

Bietenholz et al. (2011.11737)

Late phase: statistics of 294 SN remnants from Green and SNRcat:

- $L_0 \sim \mathcal{O}(10)$ Jy
- $\alpha \sim 0.5$ (spectral index)
- angular size $\sim \mathcal{O}(10)$ arcmin
- galactic coordinate
- distance $\sim \mathcal{O}(\text{kpc})$
- age (X-ray observation etc.) $\sim \mathcal{O}(10^3) - \mathcal{O}(10^5)$ years

Early phase: statistics of 262 SNe measured in the range of 2-10 GHz leads to

$$L_{\rm peak} = 10^{1.7\pm0.9}{\rm erg\ s^{-1}\ Hz^{-1}}, \qquad t_{\rm peak} = 10^{25.5\pm1.5}\ {\rm d}$$

Bietenholz et al. (2011.11737)

Late phase: statistics of 294 SN remnants from Green and SNRcat:

- $L_0 \sim \mathcal{O}(10)$ Jy
- $\alpha \sim 0.5$ (spectral index)
- angular size $\sim \mathcal{O}(10)$ arcmin
- galactic coordinate
- distance $\sim \mathcal{O}(\rm kpc)$
- age (X-ray observation etc.) $\sim \mathcal{O}(10^3) - \mathcal{O}(10^5)$ years

$$S_{\nu_a} = \frac{16\pi^2 \Gamma_a}{m_a^4\ \sigma_a} \int dx\ \rho_a\ S_{\nu_a, stim}$$

Single dish mode:

$$P_{\rm signal} \to P_{\rm signal}$$

$$P_{\rm noise} \to P_{\rm noise} \left(\frac{\theta_{\rm sig}}{\theta_{\rm res}}\right)$$

Signal of finite size, $\theta_{\rm sig}$

Interferometry mode:

$$P_{\rm signal} \to P_{\rm signal}\Theta(\lambda/B - \theta_{\rm sig})$$

$$P_{\rm noise} \to P_{\rm noise}/(\#\ \text{of meas.})^{1/2}$$

Signal of finite size, θ_{sig}

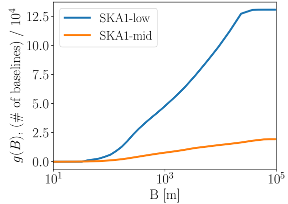

Baseline length

Interferometry mode:

$$P_{\text{signal}} \to P_{\text{signal}} \Theta(\lambda/B - \theta_{\text{sig}})$$

$$P_{\text{noise}} \to P_{\text{noise}}/(\#\text{ of meas.})^{1/2}$$

Signal of finite size, $\theta_{\rm sig}$

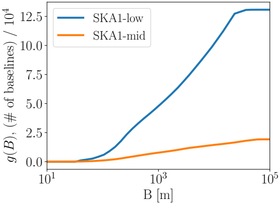

Baseline length

Interferometry mode:

$$P_{\rm signal} \to P_{\rm signal}\Theta(\lambda/B - \theta_{\rm sig})$$

$$P_{\rm noise} \to P_{\rm noise}/(\#\ \text{of meas.})^{1/2}$$

“active” baselines

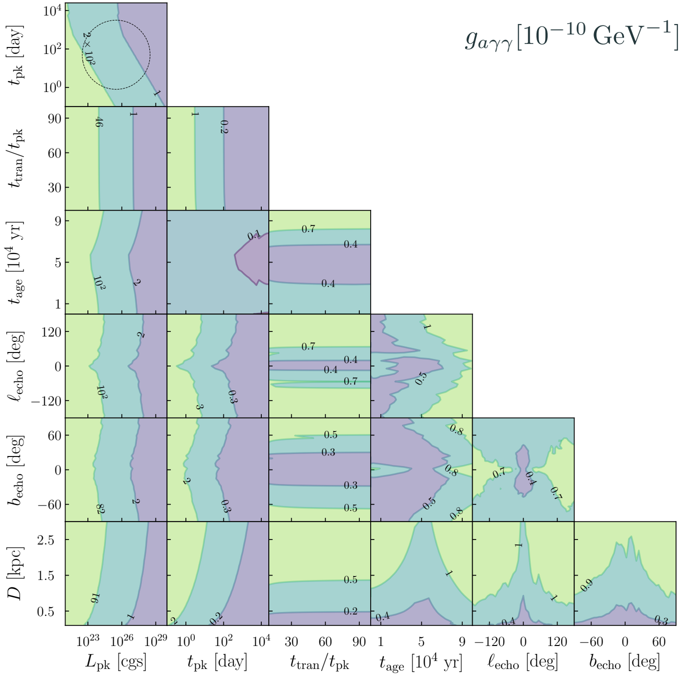
$g_{a\gamma\gamma}[10^{-10}\,\mathrm{GeV}^{-1}]$
$t_{\rm pk}$ [day]
$t_{\rm tran}/t_{\rm pk}$
$t_{\rm age}$ [10^4 yr]
$\ell_{\rm echo}$ [deg]
$b_{\rm echo}$ [deg]
D [kpc]
$L_{\rm pk}$ [cgs]

ICM – Electron density

The ICM electron density can be modeled using the double-β profile

$$n_{e,ICM} = n_{e,0} \left(f \left(1 + \frac{r^2}{r_{c1}^2} \right)^{-\frac{3\beta}{2}} + (1-f) \left(1 + \frac{r^2}{r_{c2}^2} \right)^{-\frac{3\beta}{2}} \right)$$

- "Regular" clusters (Coma-like): single beta $f = 1$
- "Cool-core" clusters (Perseus-like): double-β to account for the core

ICM – Electron density

Bonamente et al. 2006

Cluster	$\mathcal{N}$ (10^{-25} g cm^{-3})	r_s (arcsec)	n_{e0} (cm^{-3})	r_{c1} (arcsec)	β	f	r_{c2} (arcsec)	D_A Gpc
CL 0016+1609	$0.10^{+0.14}_{-0.06}$	225^{+233}_{-96}	$1.40^{+0.18}_{-0.15}\times10^{-2}$	$10.3^{+4.4}_{-2.5}$	$0.761^{+0.031}_{-0.036}$	$0.48^{+0.05}_{-0.05}$	$47.8^{+3.8}_{-3.7}$	$1.38^{+0.22}_{-0.22}$
Abell 0068	$3.29^{+7.60}_{-2.51}$	70^{+62}_{-27}	$8.89^{+1.68}_{-1.18}\times10^{-3}$	–	$0.693^{+0.026}_{-0.028}$	–	$47.8^{+2.8}_{-3.0}$	$0.63^{+0.16}_{-0.19}$
Abell 0267	$2.02^{+3.04}_{-1.24}$	75^{+50}_{-31}	$1.17^{+0.11}_{-0.10}\times10^{-2}$	–	$0.698^{+0.031}_{-0.030}$	–	$40.9^{+2.8}_{-2.8}$	$0.60^{+0.11}_{-0.09}$
Abell 0370	$1.63^{+1.80}_{-0.87}$	51^{+21}_{-13}	$5.33^{+0.58}_{-0.40}\times10^{-3}$	–	$0.740^{+0.035}_{-0.028}$	–	$55.6^{+3.1}_{-2.6}$	$1.08^{+0.19}_{-0.20}$
MS 0451.6-0305	$0.27^{+0.58}_{-0.16}$	110^{+75}_{-44}	$1.26^{+0.12}_{-0.09}\times10^{-2}$	–	$0.777^{+0.019}_{-0.019}$	–	$34.5^{+1.1}_{-1.1}$	$1.42^{+0.26}_{-0.23}$
MACS J0647.7+7015	$12.01^{+16.67}_{-8.41}$	36^{+22}_{-13}	$2.19^{+0.34}_{-0.25}\times10^{-2}$	–	$0.653^{+0.019}_{-0.017}$	–	$19.9^{+1.2}_{-1.2}$	$0.77^{+0.21}_{-0.18}$
Abell 0586	$1.78^{+1.97}_{-1.05}$	102^{+40}_{-26}	$1.83^{+0.25}_{-0.21}\times10^{-2}$	–	$0.627^{+0.017}_{-0.013}$	–	$32.0^{+1.7}_{-1.4}$	$0.52^{+0.15}_{-0.12}$
MACS J0744.8+3927	$0.27^{+0.84}_{-0.22}$	94^{+102}_{-51}	$1.14^{+0.22}_{-0.15}\times10^{-1}$	$3.4^{+0.6}_{-0.7}$	$0.635^{+0.049}_{-0.039}$	$0.93^{+0.01}_{-0.01}$	$25.8^{+4.7}_{-4.7}$	$1.68^{+0.48}_{-0.38}$
Abell 0611	$1.73^{+1.87}_{-0.90}$	64^{+15}_{-12}	$5.27^{+0.97}_{-1.00}\times10^{-2}$	$2.8^{+0.4}_{-0.3}$	$0.600^{+0.014}_{-0.008}$	$0.66^{+0.08}_{-0.07}$	$22.5^{+1.6}_{-1.2}$	$0.78^{+0.18}_{-0.18}$
Abell 0665	$0.18^{+0.14}_{-0.09}$	340^{+150}_{-86}	$9.13^{+1.34}_{-1.06}\times10^{-3}$	$3.2^{+0.8}_{-0.5}$	$0.730^{+0.015}_{-0.016}$	$0.11^{+0.10}_{-0.08}$	$64.4^{+1.7}_{-1.8}$	$0.66^{+0.09}_{-0.10}$
Abell 0697	$0.76^{+1.63}_{-0.59}$	93^{+66}_{-32}	$9.82^{+1.55}_{-1.28}\times10^{-3}$	–	$0.584^{+0.014}_{-0.016}$	–	$41.6^{+1.6}_{-1.9}$	$0.88^{+0.30}_{-0.23}$
Abell 0773	$1.22^{+1.98}_{-0.88}$	54^{+40}_{-19}	$8.04^{+0.68}_{-0.64}\times10^{-3}$	–	$0.564^{+0.020}_{-0.022}$	–	$40.2^{+2.2}_{-2.3}$	$0.98^{+0.17}_{-0.14}$
ZW 3146	$0.66^{+0.08}_{-0.05}$	121^{+4}_{-6}	$1.70^{+0.02}_{-0.03}\times10^{-1}$	$4.4^{+0.1}_{-0.1}$	$0.668^{+0.005}_{-0.004}$	$0.881^{+0.004}_{-0.003}$	$25.5^{+0.7}_{-0.4}$	$0.83^{+0.02}_{-0.02}$
MS 1054-0321	$0.04^{+0.08}_{-0.02}$	666^{+571}_{-359}	$6.15^{+0.71}_{-0.56}\times10^{-3}$	–	$1.791^{+0.148}_{-0.209}$	–	$83.7^{+4.9}_{-7.3}$	$1.33^{+0.28}_{-0.26}$
MS 1137.5+6625	$1.73^{+7.31}_{-1.40}$	16^{+18}_{-9}	$1.26^{+0.16}_{-0.11}\times10^{-2}$	–	$0.667^{+0.044}_{-0.043}$	–	$14.2^{+1.5}_{-1.3}$	$2.85^{+0.52}_{-0.63}$
MACS J1149.5+2223	$0.74^{+3.06}_{-0.50}$	110^{+46}_{-29}	$8.53^{+1.04}_{-0.89}\times10^{-3}$	–	$0.673^{+0.020}_{-0.022}$	–	$42.8^{+2.1}_{-2.4}$	$0.80^{+0.19}_{-0.16}$
Abell 1413	$0.47^{+0.58}_{-0.27}$	121^{+51}_{-47}	$3.66^{+0.65}_{-0.42}\times10^{-2}$	$6.5^{+1.5}_{-1.3}$	$0.531^{+0.018}_{-0.014}$	$0.76^{+0.02}_{-0.02}$	$39.3^{+4.5}_{-3.7}$	$0.78^{+0.18}_{-0.13}$
CL J1226.9+3332	$4.09^{+9.41}_{-3.58}$	46^{+58}_{-19}	$3.01^{+0.47}_{-0.44}\times10^{-2}$	–	$0.715^{+0.038}_{-0.038}$	–	$15.8^{+1.3}_{-1.4}$	$1.08^{+0.42}_{-0.28}$
MACS J1311.0-0310	$7.59^{+17.81}_{-7.09}$	19^{+47}_{-9}	$3.93^{+0.72}_{-0.55}\times10^{-2}$	–	$0.613^{+0.022}_{-0.020}$	–	$9.3^{+0.7}_{-0.7}$	$1.38^{+0.47}_{-0.37}$
Abell 1689	$2.68^{+1.20}_{-1.16}$	75^{+19}_{-10}	$4.054^{+0.36}_{-0.26}\times10^{-2}$	$21.7^{+0.9}_{-1.0}$	$0.873^{+0.039}_{-0.041}$	$0.87^{+0.01}_{-0.01}$	$104.9^{+5.1}_{-5.5}$	$0.65^{+0.09}_{-0.09}$
RX J1347.5-1145	$4.57^{+1.06}_{-0.86}$	47^{+5}_{-5}	$2.81^{+0.16}_{-0.12}\times10^{-1}$	$3.9^{+0.2}_{-0.1}$	$0.631^{+0.009}_{-0.008}$	$0.942^{+0.004}_{-0.004}$	$22.9^{+1.8}_{-1.4}$	$0.96^{+0.06}_{-0.08}$
MS 1358.4+6245	$0.58^{+0.21}_{-0.19}$	90^{+26}_{-18}	$9.62^{+0.79}_{-0.78}\times10^{-2}$	$3.3^{+0.2}_{-0.2}$	$0.675^{+0.017}_{-0.016}$	$0.934^{+0.003}_{-0.003}$	$37.2^{+1.7}_{-1.9}$	$1.13^{+0.09}_{-0.10}$
Abell 1835	$0.28^{+0.10}_{-0.03}$	150^{+11}_{-11}	$1.10^{+0.05}_{-0.02}\times10^{-1}$	$9.3^{+0.2}_{-0.2}$	$0.798^{+0.013}_{-0.017}$	$0.940^{+0.001}_{-0.001}$	$63.7^{+1.5}_{-1.6}$	$1.07^{+0.02}_{-0.08}$
MACS J1423.8+2504	$1.83^{+0.02}_{-0.07}$	33^{+1}_{-1}	$1.60^{+0.02}_{-0.08}\times10^{-1}$	$4.2^{+0.1}_{-0.1}$	$0.721^{+0.012}_{-0.008}$	$0.975^{+0.001}_{-0.001}$	$36.7^{+0.9}_{-0.7}$	$1.49^{+0.06}_{-0.03}$
Abell 1914	$5.79^{+2.60}_{-1.85}$	81^{+14}_{-11}	$1.72^{+0.13}_{-0.08}\times10^{-2}$	$6.6^{+0.6}_{-0.8}$	$0.899^{+0.007}_{-0.012}$	$0.008^{+0.018}_{-0.008}$	$68.3^{+0.7}_{-1.0}$	$0.44^{+0.04}_{-0.05}$
Abell 1995	$0.07^{+0.06}_{-0.04}$	359^{+205}_{-117}	$9.35^{+0.74}_{-0.56}\times10^{-3}$	$31.2^{+3.0}_{-3.5}$	$1.298^{+0.062}_{-0.096}$	$0.462^{+0.033}_{-0.033}$	$83.5^{+3.7}_{-7.1}$	$1.19^{+0.15}_{-0.14}$
Abell 2111	$0.47^{+2.74}_{-0.38}$	172^{+354}_{-107}	$5.99^{+1.05}_{-0.79}\times10^{-3}$	–	$0.600^{+0.026}_{-0.025}$	–	$50.4^{+3.8}_{-3.5}$	$0.64^{+0.20}_{-0.17}$
Abell 2163	$0.26^{+0.12}_{-0.09}$	390^{+87}_{-52}	$1.09^{+0.07}_{-0.04}\times10^{-2}$	$4.0^{+1.3}_{-0.7}$	$0.560^{+0.004}_{-0.005}$	$0.022^{+0.037}_{-0.022}$	$66.8^{+0.9}_{-0.8}$	$0.52^{+0.04}_{-0.05}$
Abell 2204	$0.92^{+0.30}_{-0.15}$	120^{+13}_{-18}	$2.01^{+0.12}_{-0.09}\times10^{-1}$	$7.5^{+0.3}_{-0.3}$	$0.710^{+0.031}_{-0.025}$	$0.960^{+0.003}_{-0.004}$	$67.4^{+2.0}_{-1.8}$	$0.61^{+0.06}_{-0.07}$
Abell 2218	$1.02^{+0.70}_{-0.60}$	110^{+35}_{-22}	$7.02^{+0.66}_{-0.66}\times10^{-3}$	–	$0.739^{+0.014}_{-0.017}$	–	$68.3^{+1.7}_{-2.1}$	$0.66^{+0.14}_{-0.11}$
RX J1716.4+6708	$0.34^{+3.38}_{-0.30}$	146^{+545}_{-106}	$1.94^{+0.61}_{-0.40}\times10^{-2}$	–	$0.589^{+0.042}_{-0.035}$	–	$12.3^{+2.0}_{-1.7}$	$1.04^{+0.51}_{-0.43}$
Abell 2259	$0.65^{+1.15}_{-0.54}$	141^{+155}_{-56}	$9.29^{+2.97}_{-1.71}\times10^{-3}$	–	$0.560^{+0.025}_{-0.024}$	–	$41.0^{+3.9}_{-2.8}$	$0.58^{+0.29}_{-0.25}$
Abell 2261	$1.36^{+0.85}_{-0.85}$	68^{+25}_{-15}	$4.16^{+0.54}_{-0.63}\times10^{-2}$	$10.0^{+1.9}_{-1.7}$	$0.628^{+0.025}_{-0.022}$	$0.77^{+0.04}_{-0.05}$	$37.8^{+6.5}_{-5.2}$	$0.73^{+0.20}_{-0.13}$
MS 2053.7-0449	$0.26^{+1.41}_{-0.22}$	40^{+64}_{-22}	$9.22^{+1.08}_{-0.92}\times10^{-3}$	–	$0.522^{+0.048}_{-0.042}$	–	$10.8^{+1.9}_{-1.7}$	$2.48^{+0.41}_{-0.44}$

ICM – Magnetic field

We follow previous studies and assume a B_{ICM} profile

$$B_{ICM} = B_{ref} \left(\frac{n_e(r)}{n_e(r_{ref})} \right)^{\eta}$$

with two profiles similar to Perseus, and one similar to Coma

Model	r_{ref}	B_{ref}	η
A	0 kpc	25 μG	0.7
B	25 kpc	7.5 μG	0.5
C	0 kpc	4.7 μG	0.5

Bonafede et al. 2010, Feretti et al. 2012, Reynolds et al. 2019, Angus et al. 2014

ICM – Magnetic field

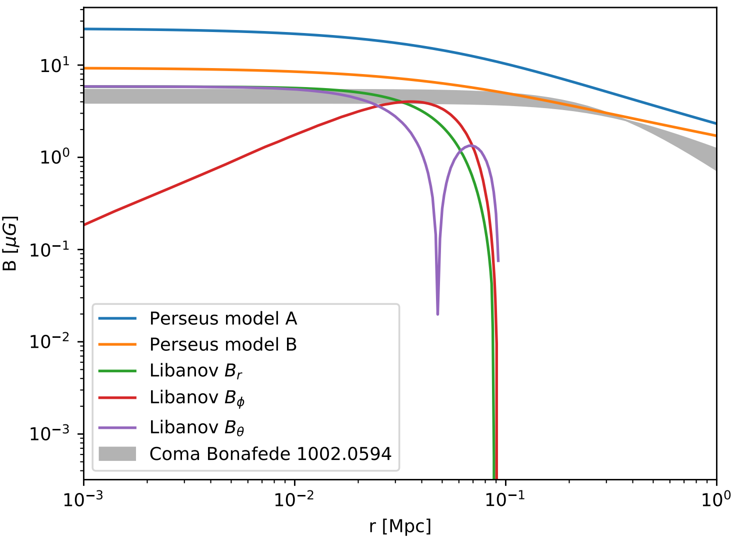

ICM – Magnetic field

We follow previous studies and assume a B_{ICM} profile

$$B_{ICM} = B_{ref} \left(\frac{n_e(r)}{n_e(r_{ref})} \right)^{\eta}$$

with two profiles similar to Perseus, and one similar to Coma

Model	r_{ref}	B_{ref}	η
A	0 kpc	25 μG	0.7
B	25 kpc	7.5 μG	0.5
C	0 kpc	4.7 μG	0.5
no ICM	n/a	0 μG	n/a

Bonafede et al. 2010, Feretti et al. 2012,
Reynolds et al. 2019, Angus et al. 2014,
Libanov and Troitsky 2020

$P_{a\gamma}(x)$

$$
\begin{aligned}
P_{a\gamma} &= \frac{(2\Delta)^2}{k^2} \sin^2\left(\frac{kx}{2}\right) \\
&= \frac{g_{a\gamma}^2 B^2}{g_{a\gamma}^2 B^2 + (m_a^2 - m_\gamma^2)^2/(4\omega^2)} \sin^2\left(\left(\frac{1}{2}\sqrt{g_{a\gamma}^2 B^2 + \frac{(m_a^2 - m_\gamma^2)^2}{4\omega^2}}\right) x\right),
\end{aligned}
$$

- "Baseline": intergalactic medium (IGM)
- "Baseline specs": B, n_e

IGM – magnetic field strength

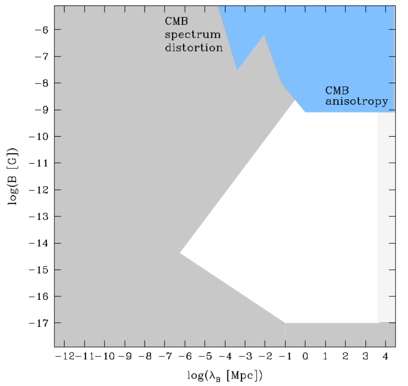

IGM magnetic field:

- CMB anisotropies, lack of Faraday rotation of of quasars, $B_{IGM} \lesssim \mathrm{nG}$.

IGM – magnetic field strength

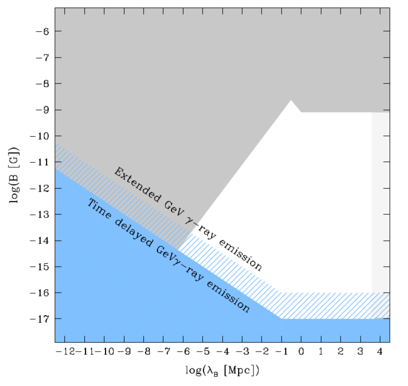

IGM magnetic field:

- CMB anisotropies, lack of Faraday rotation of of quasars, $B_{IGM} \lesssim \mathrm{nG}$.
- Non-observation of cascade of TeV γ-ray, $B_{IGM} \gtrsim 10^{-16}$ G.

IGM – magnetic field strength

Note that in the oscillation formula,

$$P_0 = \frac{g_{a\gamma}^2 B^2}{g_{a\gamma}^2 B^2 + (m_a^2 - m_\gamma^2)^2/(4\omega^2)} \sin^2\left(\left(\frac{1}{2}\sqrt{g_{a\gamma}^2 B^2 + \frac{(m_a^2 - m_\gamma^2)^2}{4\omega^2}}\right) z\right),$$

$(g_{a\gamma} B)$ shows up hand-in-hand.

- So what we bound in IGM is actually on $(g_{a\gamma} B)$.
- In this work, we take common benchmark $B_{IGM} \sim \mathrm{nG}$.
- Future detection of $B_{IGM} < \mathrm{nG}$ will rescale the bounds on $g_{a\gamma}$ as B_{IGM}/nG.

c.f. Durrer and Neronov 2013, Vachaspati 2010

IGM – electron density

$$P_0 = \frac{g_{a\gamma}^2 B^2}{g_{a\gamma}^2 B^2 + (m_a^2 - m_\gamma^2)^2/(4\omega^2)} \sin^2\left(\left(\frac{1}{2}\sqrt{g_{a\gamma}^2 B^2 + \frac{(m_a^2 - m_\gamma^2)^2}{4\omega^2}}\right) z\right),$$

At low redshift, $z < 0.5$, *Nicastro et al. Nature 2018, Martizzi et al. MNRAS, 2019*

$$\text{baryons} \begin{cases} \text{Lyman-}\alpha\text{ forest, } 28 \pm 11\% \text{ mass, } \gtrsim 90\% \text{ volume} \\ \text{warm-hot intergalactic matter, } \lesssim 10\% \text{ volume} \end{cases}$$

- $\bar{n}_{e,Ly\alpha} \approx 6.5 \times 10^{-8}\ \text{cm}^{-3}$

IGM – electron density

At low redshift, $z < 0.5$, *Nicastro et al. Nature 2018, Martizzi et al. MNRAS, 2019*

$$\text{baryons} \begin{cases} \text{Lyman-}\alpha \text{ forest, } 28 \pm 11\% \text{ mass, } \gtrsim 90\% \text{ volume} \\ \text{warm-hot intergalactic matter, } \lesssim 10\% \text{ volume} \end{cases}$$

- $\bar{n}_{e,Ly\alpha} \approx 6.5 \times 10^{-8}\ \mathrm{cm}^{-3}$

Simulation shows at $z < 1$

$$\text{Lyman-}\alpha \begin{cases} \text{underdense patches, a.k.a. cosmic voids} & \sim 30 - 50\% \text{ vol.} \\ \text{2D structures, a.k.a. sheets} & \sim 30 - 50\% \text{ vol.} \end{cases}$$

- $n_e \approx 1.6 \times 10^{-8}\ \mathrm{cm}^{-3}$ (cosmic voids)
- $n_e \approx 3.0 \times 10^{-8}\ \mathrm{cm}^{-3}$ (sheets)

Late vs Early

- The theory parameters:

$$\theta = (\underbrace{m_a, g_{a\gamma}}_{\text{axion}}; \underbrace{H_0, \Omega_\Lambda}_{\Lambda CDM}; \underbrace{m_{10}}_{\text{nuisance}})$$

- The likelihoods:

$$\mathcal{L} \equiv \mathcal{L}_{\text{Pan}} \cdot \mathcal{L}_{\text{cluster}} \cdot \ldots$$

Late vs Early

- The theory parameters:

$$\theta = \big(\underbrace{m_a, g_{a\gamma}}_{\text{axion}};\ \underbrace{H_0, \Omega_\Lambda}_{\Lambda CDM};\ \underbrace{m_{10}, r_s^{drag}}_{\text{nuisance}}\big)$$

- The likelihoods:

$$\mathcal{L}_{\text{early}} \equiv \mathcal{L}_{\text{Pan}} \cdot \mathcal{L}_{\text{cluster}} \cdot \mathcal{L}_{\text{BAO}} \cdot \mathcal{L}_{\text{Plank}}$$
$$\mathcal{L}_{\text{late}} = \mathcal{L}_{\text{Pan}} \cdot \mathcal{L}_{\text{cluster}} \cdot \mathcal{L}_{\text{BAO}} \cdot \mathcal{L}_{\text{SH0ES}} \cdot \mathcal{L}_{\text{TD}}$$

Late vs Early

- The theory parameters:

$$\theta = \big(\underbrace{m_a, g_{a\gamma}}_{\text{axion}};\ \underbrace{H_0, \Omega_\Lambda}_{\Lambda CDM};\ \underbrace{m_{10}, r_s^{drag}}_{\text{nuisance}}\big)$$

- The likelihoods:

$$\mathcal{L}_{\text{early}} \equiv \mathcal{L}_{\text{Pan}} \cdot \mathcal{L}_{\text{cluster}} \cdot \mathcal{L}_{\text{BAO}} \cdot \mathcal{L}_{\text{Plank}}$$

$$\mathcal{L}_{\text{late}} = \mathcal{L}_{\text{Pan}} \cdot \mathcal{L}_{\text{cluster}} \cdot \mathcal{L}_{\text{BAO}} \cdot \mathcal{L}_{\text{SH0ES}} \cdot \mathcal{L}_{\text{TD}}$$

- Production runs:

$$\begin{Bmatrix} \text{early} \\ \text{late} \end{Bmatrix} \otimes \begin{Bmatrix} n_e^{IGM} = 1.6 \times 10^{-8}\ \text{cm}^{-3} \\ n_e^{IGM} = 3.0 \times 10^{-8}\ \text{cm}^{-3} \end{Bmatrix} \otimes \begin{Bmatrix} \text{ICM A} \\ \text{ICM B} \\ \text{ICM C} \\ \text{no ICM} \end{Bmatrix}$$

Other data sets (priors)

- SH0ES:

$$-2\ln\mathcal{L}_{SH0ES} = \sum_{i=1}^{19}\left(\frac{m_{10,i}^{SH0ES} - m_{10}}{\sigma_i^{SH0ES}}\right)^2$$

- TDCOSMO:

$$-2\ln\mathcal{L}_{TDCOSMO} = \left(\frac{H_0^{TD} - H_0}{\sigma^{TD}}\right)^2$$

- BAO: (BOSS DR12 CMASS and LOWZ; 6dFGS, MGS)

$$-2\ln\mathcal{L}_{BAO} = \sum_{i,j}\Delta_i C_{ij}^{BAO}\Delta_j$$

$$\Delta_i = (Q_i^{BAO} - Q^{\Lambda CDM}(z_i;\Omega_\Lambda, H_0, r_s^{drag}))$$

- Planck

$$-2\ln\mathcal{L}_{Pl} = \left(\frac{r_s^{Pl} - r_s}{\sigma^{Pl}}\right)^2$$